PNAS RESEARCH ARTICLE | MEDICAL SCIENCES

CLCF1 inhibits energy expenditure via suppressing brown fat thermogenesis

Youwen Yuan[a,b,c,1], Kangli Li[d,1], Xueru Ye[a,b,c,1], Shiyi Wen[e,f,1], Yanan Zhang[a,b,c], Fei Teng[a,b,c], Xuan Zhou[a,b,c], Yajuan Deng[a,b,c], Xiaoyu Yang[a,b,c], Weiwei Wang[a,b,c], Jiayang Lin[a,b,c], Shenjian Luo[a,b,c], Peizhen Zhang[a,b,c], Guojun Shi[e,f,2], and Huijie Zhang[a,b,c,2]

Edited by Christian Wolfrum, Eidgenossische Technische Hochschule Zurich, Zurich Schwerzenbach, Switzerland; received July 5, 2023; accepted November 17, 2023 by Editorial Board Member David J. Mangelsdorf

Brown adipose tissue (BAT) is the main site of nonshivering thermogenesis which plays an important role in thermogenesis and energy metabolism. However, the regulatory factors that inhibit BAT activity remain largely unknown. Here, cardiotrophin-like cytokine factor 1 (CLCF1) is identified as a negative regulator of thermogenesis in BAT. Adenovirus-mediated overexpression of CLCF1 in BAT greatly impairs the thermogenic capacity of BAT and reduces the metabolic rate. Consistently, BAT-specific ablation of CLCF1 enhances the BAT function and energy expenditure under both thermoneutral and cold conditions. Mechanistically, adenylate cyclase 3 (ADCY3) is identified as a downstream target of CLCF1 to mediate its role in regulating thermogenesis. Furthermore, CLCF1 is identified to negatively regulate the PERK-ATF4 signaling axis to modulate the transcriptional activity of ADCY3, which activates the PKA substrate phosphorylation. Moreover, CLCF1 deletion in BAT protects the mice against diet-induced obesity by promoting BAT activation and further attenuating impaired glucose and lipid metabolism. Therefore, our results reveal the essential role of CLCF1 in regulating BAT thermogenesis and suggest that inhibiting CLCF1 signaling might be a potential therapeutic strategy for improving obesity-related metabolic disorders.

CLCF1 | brown adipose tissue | thermogenesis | obesity

Significance

The essence of obesity is the imbalance between energy intake and consumption. Brown adipose tissue (BAT) has a thermogenic effect due to its numerous mitochondria, which promotes energy expenditure and nonshivering thermogenesis. Promoting the thermogenesis of BAT is a well-accepted strategy for improving energy balance. Here, we identify CLCF1 as a negative regulator of thermogenesis in BAT. CLCF1 deletion in BAT shows enhanced thermogenesis and attenuation of diet-induced obesity. Mechanistically, CLCF1 suppresses the PERK-ATF4 pathway and further inhibits ADCY3 transcriptional activity and PKA signaling, which impairs thermogenesis of BAT. Thus, this study provides the evidence for the role of CLCF1 signaling in modulating BAT thermogenesis, which might help to uncover the pathophysiological mechanisms of obesity and associated metabolic disorders.

Brown adipose tissue (BAT) is the major site of adaptive thermogenesis which plays a critical roles in whole-body energy balance and fuel metabolism in mammals (1, 2). BAT contains a large number of multilocular lipid droplets and mitochondria and actively takes up glucose and fatty acids for oxidation by driving uncoupling respiration mediated by uncoupling protein 1 (UCP1) located in mitochondria (1–4). A growing body of evidence from both animal and human studies suggests that high BAT thermogenic activity and capacity is associated with resistance to obesity and related metabolic alterations (4–9). It is attracting increasing interest to promote BAT thermogenesis for counteracting the hypercaloric state of obesity and improving metabolic disorders. However, the mechanisms of regulating the thermogenic activity of BAT remain largely unclear.

The interleukin-6 (IL-6) family of cytokines is a group of proteins that play pivotal roles in various physiological processes, which has been extensively studied over the past few decades (10). Previous studies have shown that some members of the IL-6 family are involved in decreasing body weight and energy expenditure (11–16). Currently, it has been established that some of those cytokines play roles in regulating the energy homeostasis by inhibiting appetite with the subsequent changes in fat metabolism, including IL-6, cardiotrophin 1 (CT1), ciliary neurotrophic factor (CNTF), and leukemia inhibitory factor (LIF) (11–17). Besides, our previous study also revealed that circulating LIF levels in people with obesity were positively associated with hepatic steatosis, and adenoviruses-mediated increasing of circulating LIF reduced hepatic lipid deposition and improved glucose homeostasis in mice (18). In addition, IL27, another member of the IL-6 family, was recently identified to promote adipocyte thermogenesis and improve systemic metabolic homeostasis (17). However, whether the IL6 family of cytokines could directly target BAT to regulate thermogenesis and energy metabolism independent of its effect on the central nervous system remains unclear.

Cardiotrophin-like cytokine factor 1 (CLCF1) was identified as another member of the IL6 family to promote the recruitment and phosphorylation of gp130 and LIFR through binding to the ciliary neurotrophic factor receptor (CNTFR) in tumorogenesis (19–22). In addition, mutations in the CLCF1 gene lead to cold-induced sweating syndrome (CISS) with dysregulated body temperature (23). However, the role of CLCF1 in energy homeostasis remains unclear. In this study, we investigated the role of CLCF1 in regulating BAT thermogenesis as well as its underlying mechanisms in the development of obesity. Our data reveal that CLCF1 is a negative regulator in BAT thermogenesis and

The authors declare no competing interest.

This article is a PNAS Direct Submission. C.W. is a guest editor invited by the Editorial Board.

[1]Y.Y., K.L., X. Ye, and S.W. contributed equally to this work.

[2]To whom correspondence may be addressed. Email: huijiezhang2005@126.com or shigj6@mail.sysu.edu.cn.

This article contains supporting information online at https://www.pnas.org/lookup/suppl/doi:10.1073/pnas.2310711121/-/DCSupplemental.

Published January 8, 2024.

energy expenditure, and inhibition of CLCF1 in BAT protects mice against diet-induced obesity, suggesting the potential role for CLCF1 in BAT in regulating energy and metabolic balance.

Results

Expression Levels of CLCF1 in BAT under Normal and Cold Exposure Conditions. To identify IL-6 family members in BAT that respond to thermogenesis, we performed RNA sequencing analysis of BAT from C57BL/6 mice after 1 d of cold challenge at 8 °C and their C57BL/6 mice counterparts housed at 30 °C for 1 d. Gene expression analysis showed 1766 genes that were up-regulated and 2779 genes that were down-regulated after cold challenge (Fig. 1*A*), including *Ucp1,* deiodinase 2 (*Dio2*), and elongation of very-long-chain fatty acids (*Elovl3*) (Fig. 1*A*). Interestingly, Gene Ontology (GO) analysis of the transcriptomic profiles on differentially expressed genes indicated that both "fatty acid metabolic process" and "regulation of inflammatory response" pathways were enriched under cold exposure (Fig. 1*B*). Previous reports demonstrated that IL-6 family genes were critical in mediating thermogenic response to cold exposure in adipose tissue (17, 24). Thus, we analyzed the mRNA expression of well-recognized cytokines and the corresponding receptors of the IL-6 family members in BAT. Interestingly, CLCF1 stood out due to its dynamic expression pattern in BAT under cold exposure (Fig. 1*C*). The protein expression levels of CLCF1 in different tissues were detected, showing that CLCF1 was mainly expressed in the heart, muscle, liver, BAT, and jejunum, with BAT as the most abundant compared with other tissues analyzed. However, CLCF1 protein levels in inguinal white adipose tissue (iWAT) and epididymal white adipose tissue (eWAT) were relatively low (Fig. 1*D*). Consistent with the CLCF1 expression pattern, the mRNA expression of *Cntfr* was the most abundant in BAT compared with other tissues analyzed, while the *Lifr* and *gp130*, the other two components forming a trimeric complex with CNTFR, showed different expression patterns compared with CLCF1 (*SI Appendix*, Fig. S1 *A–C*). In addition, we further retrieved the RNA sequencing data of human preadipocytes on differentiation at day 0 and day 21 from the public database (GSE97205). It showed that the mRNA expression level of CLCF1 was down-regulated while UCP1 was up-regulated during the differentiation of human brown adipocytes (*SI Appendix*, Fig. S1*D*). In contrast, the mRNA expression level of UCP1 was comparable during the differentiation of human white adipocytes (*SI Appendix*, Fig. S1*D*), although the mRNA expression of CLCF1 was also reduced. To explore the physiological function of CLCF1 in BAT, the mRNA and protein expression levels of CLCF1 in BAT were analyzed in mature adipocytes (Ad) and stormal vascular fractions (SVFs), showing that CLCF1 was mainly expressed in mature adipocytes (Fig. 1 *E* and *F*). However, there were no differences between Ads and SVFs in white adipose tissue (*SI Appendix*, Fig. S1 *E* and *F*). Further, reduced CLCF1 mRNA and protein levels in BAT were confirmed under cold exposure condition, as well as cold-mimic condition with CL316,243 treatment (Fig. 1 *G–J*). These results show that CLCF1 is highly expressed in BAT and is responsive to adaptive thermogenesis, suggesting that CLCF1 might play important roles in energy homeostasis.

CLCF1 Suppresses the Thermogenic Activity of BAT in Mice. To investigate the potential impact of CLCF1 signaling on BAT function, adenoviruses carrying CLCF1 coding sequence (Ad-CLCF1) or control gene (Ad-green fluorescent protein, Ad-GFP) were administered into BAT of C57BL/6 mice (Fig. 2*A*). The protein expression levels of CLCF1 were significantly increased in BAT, but not in iWAT and eWAT, followed by exposure to 8 °C for 7 d (Fig. 2 *B* and *C*). Ad-CLCF1-treated mice failed to maintain their core body temperature (Fig. 2*D*) and showed less weight loss after cold exposure without changes in food intake compared with the control mice (Fig. 2 *E* and *F*). Ad-CLCF1-treated mice also showed reductions in their O_2 consumption, CO_2 emission and heat production without alterations in the respiratory exchange ratio (RER) (Fig. 2 *G–J*). These data suggest that increased CLCF1 expression in BAT impairs adaptation to cold exposure. With CLCF1 overexpression in BAT, BAT mass was significantly increased (Fig. 2*K*), BAT color became lighter in brown (Fig. 2*L*), and the proportion of large adipocytes in BAT was increased (Fig. 2 *M* and *N*) with more lipid content (Fig. 2*O*). Consistently, reduced mRNA and protein levels of UCP1 were observed in BAT from Ad-CLCF1-treated mice (Fig. 2 *P* and *Q*).

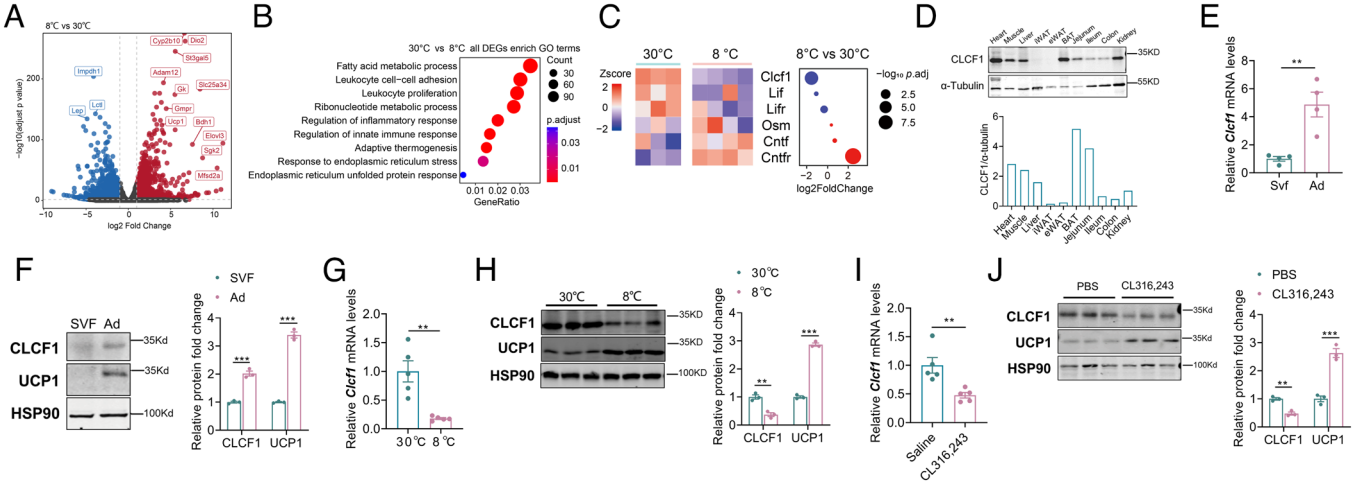

Fig. 1. CLCF1 was mainly expressed in BAT and down-regulated by cold and CL316,243 stimulation. (*A*) Volcano plot representing the up-regulated and down-regulated genes in BAT, assessed by RNA-seq (8 °C, n = 4; 30 °C, n = 3) (|log2(Fold Change)| >1, P_{adj} < 0.05). (*B*) GO biological process analysis of RNA-seq (8 °C, n = 4; 30 °C, n = 3). (*C*) Heat map representation of top-ranked IL-6 family genes and its receptor deferentially expressed (8 °C, n = 4; 30 °C, n = 3). (*D*) The protein levels of CLCF1 in different tissues of 8-wk-old male C57BL/6J mice mice. (*E*) The mRNA levels of CLCF1 in mature adipocytes and SVF of BAT from male C57BL/6J mice (n = 4). (*F*) The protein levels of CLCF1 in mature adipocytes and SVF of BAT (*Left*) and quantification of protein levels (*Right*) (n = 3 biological replicates). (*G*) The mRNA levels and (*H*) the protein levels (*Left*) and quantification of protein levels (*Right*) of CLCF1 in BAT from 8-wk-old male C57BL/6J mice housed at 30 °C or 8 °C for 1d (*G*, n = 5; *F* and *H*, n = 3). (*I*) The mRNA levels and (*J*) the protein levels (*Left*) and quantification of protein levels (*Right*) of CLCF1 in BAT from 8-wk-old male C57BL/6J mice injected intraperitoneally with CL316,243 for 1 d (*I*, n = 5; *J*, n = 3). Data are presented as mean ± SEM and ***P* < 0.01 and ****P* < 0.001 by unpaired two-tailed Student's *t* tests (*E–J*).

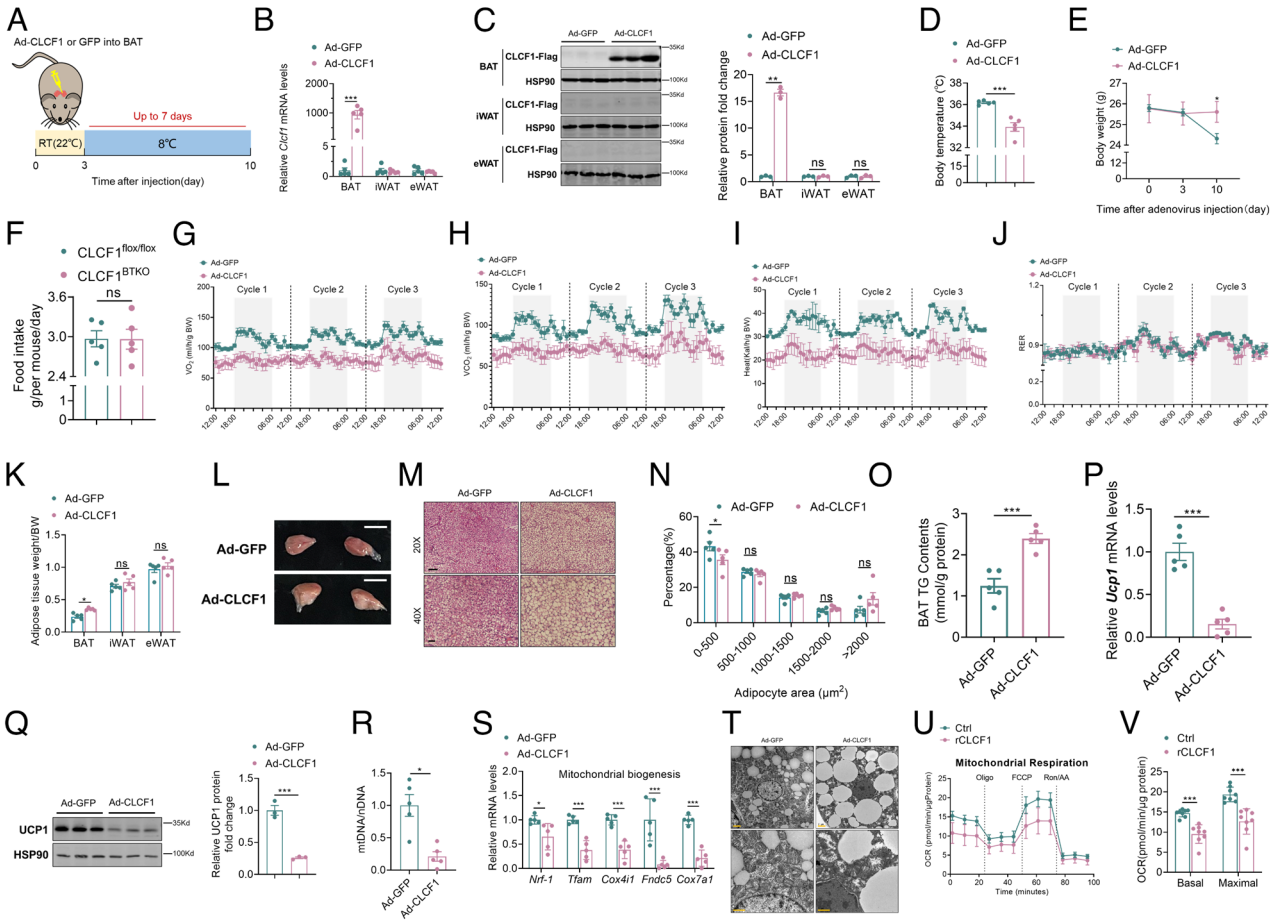

Fig. 2. Overexpression of CLCF1 impaired the thermogenic function of BAT. (*A*) The BAT of 8-wk-old male C57BL/6J mice housed at room temperature was injected with adenovirus. After 3 d of adenovirus injection, mice were transferred to 8 °C for up to 7 d. (*B*) The mRNA levels and (*C*) the protein levels (*Left*) and quantification of protein levels (*Right*) of CLCF1 in BAT, iWAT, and eWAT (*B*, n = 5; *C*, n = 3). (*D*) Core body temperatures (n = 5). (*E*) Body weight (n = 5). (*F*) Averaged daily food intake (n = 5). (*G*) Oxygen consumption, (*H*) carbon dioxide production, (*I*) energy expenditure, and (*J*) respiratory exchange ratio (n = 4). (*K*) Relative adipose tissue weight (normalized to body weight, n = 5). (*L*) Representative photographs of BAT. (*M*) Representative H&E stains of BAT (*Top*, Scale bar, 50 μm; *Bottom*, Scale bar, 25 μm.) and (*N*) distribution of adipocyte area (n = 5). (*O*) BAT triglyceride contents (n = 5). (*P*) The mRNA levels and (*Q*) the protein levels (*Left*) and quantification of protein levels (*Right*) of UCP1 in BAT (*P*, n = 5; *Q*, n = 3). (*R*) Relative mitochondrial DNA (mtDNA) levels (n = 5). (*S*) The mRNA levels of mitochondrial biogenesis genes in BAT (n = 5). (*T*) Representative TEM images of mitochondria in BAT. (*Top*, Scale bar, 2 μm; *Bottom*, Scale bar, 1 μm.) (*U*) Oxygen consumption profiles of brown adipocytes following stimulation by the indicated agents. (*V*) Bar graphs represent quantification of basal and maximal oxygen consumption. Data are presented as mean ± SEM and $^{*}P < 0.05$, $^{**}P < 0.01$, and $^{***}P < 0.001$. Unpaired two-tailed Student's *t* tests were performed in *B–F*, *K*, and *N–S*. Two-way ANOVA tests were performed in *V*.

BAT is highly enriched in mitochondria, and the analysis of relative mitochondrial copy number, mitochondrial biogenesis–related gene expression, and electron microscopy indicate the reduction in mitochondrial content in BAT of Ad-CLCF1-treated mice (Fig. 2 *R–T*). To further analyze the role of CLCF1 in regulating mitochondrial function, the SVFs from BAT of wild-type (WT) mice were isolated and differentiated into mature adipocytes, followed by treatment with recombinant CLCF1 protein (rCLCF1). The data show reduced levels of both basal and maximal mitochondrial respiration in adipocytes treated with rCLCF1 by measuring the oxygen consumption rate (OCR) (Fig. 2 *U* and *V*). To evaluate the function of CLCF1 in human adipocytes, primary adipocytes were isolated from collected human visceral adipose tissues (SAT) followed by induction of differentiation into brown adipocytes. Interestingly, our results show that treatment of rCLCF1 reduced the mRNA expression levels of UCP1 in either undifferentiated preadipocytes or differentiated human brown adipocytes (*SI Appendix*, Fig. S2*A*). Consistently, the relative mitochondrial DNA (mtDNA) levels and the mitochondrial biogenesis gene expression levels were significantly suppressed by rCLCF1 in undifferentiated preadipocytes and differentiated human brown adipocytes, suggesting the role of CLCF1 in inhibiting thermogenesis in human adipocytes (*SI Appendix*, Fig. S2 *B* and *C*). As the expression level of CLCF1 in WAT was relatively low under physiological conditions, we injected adenovirus into iWAT of WT mice and transferred them to 8 °C cold exposure for another 7 d, aiming to test whether increased CLCF1 expression has any effect on the remodeling of white fat. Although the injection of Ad-CLCF1 led to elevated expression of CLCF1 in iWAT (*SI Appendix*, Fig. S3 *A* and *B*), Ad-CLCF1-treated mice exhibited no differences in body weight, metabolic rates (oxygen consumption, CO_2 emission, heat production, and RER), body temperature, iWAT mass, and the mRNA abundance of thermogenic genes compared with the control mice (*SI Appendix*, Fig. S3 *C–J*).

Collectively, these results suggest that increased CLCF1 expression in BAT leads to cold intolerance, reduced energy expenditure, and impaired mitochondrial function and that CLCF1 serves as a suppressor of adaptive thermogenesis in BAT.

CLCF1 Deletion in BAT Promotes Adaptive Thermogenesis. BAT consists of different cell types, such as adipocytes, endothelial cells, neuronal cells and immune cells, etc. (25). As CLCF1 was mainly expressed in mature adipocytes compared with SVFs of BAT (Fig. 1 *E* and *F*), we hypothesized that adipocytes in BAT play important roles in thermogenesis compared with the control mice.

Thus, we crossed *Clcf1*$^{fl/fl}$ mice with *Ucp1*-iCre mice to generate brown adipocyte–specific *Clcf1* knockout mice (*Clcf1*^{BTKO}), with *Clcf1*$^{fl/fl}$ mice as the control (*SI Appendix*, Fig. S4 *A* and *B*). The mRNA expression levels of *Clcf1* were significantly decreased in BAT, but not in iWAT, of *Clcf1*^{BTKO} mice (*SI Appendix*, Fig. S4*C*). No significant difference in body weight, body temperature and metabolic rates were observed between 10-week-old *Clcf1*^{BTKO} and their *Clcf1*^{flf}counterparts fed a normal chow diet (NCD) under room temperature. (*SI Appendix*, Fig. S5 *A–F*). When they were maintained under a thermoneutral condition at 30 °C for 10 d, core body temperature was significantly increased in *Clcf1*^{BTKO} mice compared with the control mice (Fig. 3*A*), while the body weight, food intake, and adipose tissue weight showed no differences between two groups (*SI Appendix*, Fig. S6 *A–C*). Notably, more multilocular adipocytes and increased UCP1 protein levels in BAT were observed from *Clcf1*^{BTKO} mice (Fig. 3 *B–E*). Besides, the relative mitochondrial copy number (Fig. 3*F*) and the expression levels of several mitochondrial biogenesis genes (Fig. 3*G*) in BAT of *Clcf1*^{BTKO} mice were significantly increased. Furthermore, after 2 d of cold exposure at 8 °C, *Clcf1*^{BTKO} mice displayed elevated body temperature (Fig. 3*H*) and browner BAT (Fig. 3*I*), without differences in body weight, food intake, and adipose tissue weight (*SI Appendix*, Fig. S6 *D–F*). Besides, *Clcf1*^{BTKO} mice showed increased O_2 consumption, CO_2 emission, and heat production compared with the control mice (Fig. 3 *J–L*), while there was no apparent difference in RER between groups (Fig. 3*M*). In addition, BAT adipocytes in *Clcf1*^{BTKO} mice were smaller in size with more multilocular lipid droplets compared with their *Clcf1*$^{fl/fl}$ littermates (Fig. 3*N*), whereas iWAT adipocytes showed no apparent differences between groups (*SI Appendix*, Fig. S6 *G* and *H*). Increased mRNA levels of thermogenic genes and UCP1 protein levels in *Clcf1*^{BTKO} mice were also confirmed under cold exposure (Fig. 3 *O* and *P*). Moreover, assays on relative mitochondrial copy number, mitochondrial biogenesis gene expression levels, and electron microscopy confirmed the improved mitochondrial content and function in BAT of *Clcf1*^{BTKO} mice (Fig. 3 *Q–S*). These results indicate that CLCF1 deletion in BAT promotes adaptive thermogenesis.

CLCF1 Suppresses the Thermogenic Program via ADCY3. To identify the candidate genes regulated by CLCF1 that are involved in regulating thermogenesis, we analyzed the overlapped genes in BATs differentially expressed under cold exposure vs. thermoneutral conditions in WT mice and from *Clcf1*^{BTKO} vs. *Clcf1*$^{fl/fl}$ mice both housed at thermoneutral condition (Fig. 4*A*). Notably, among the overlapped genes, adenylate cyclase 3 (ADCY3) was among the top up-regulated genes with CLCF1 deficiency (Fig. 4*B*). Then, we confirmed the elevated expression of ADCY3 in *Clcf1*^{BTKO} mice at both mRNA and protein levels (Fig. 4 *C* and *D* and *SI Appendix*, Fig. S7 *A* and *B*). Consistently, ADCY3 expression was also suppressed by CLCF1 overexpression (*SI Appendix*, Fig. S7 *C* and *D*). ADCY3 is mainly located on the cell membrane (26), which was confirmed by immunofluorescence staining (Fig. 4*E*). Moreover, our data show that CL316,243 treatment, which mimics cold exposure, did not affect plasma membrane distribution of ADCY3 in primary brown adipocytes (Fig. 4*F*). Reports have shown that Protein Kinase A (PKA) activation responds to cold stimulation, which mediates the thermogenic effect of BAT by epinephrine or CL316,243 treatment (1, 27). ADCY3 catalyzes the synthesis of cyclic AMP (cAMP), which controls PKA signaling (26–29). Thus, we analyzed PKA signaling and showed that the PKA pathway as well as ADCY3 mRNA transcription were activated in BAT from

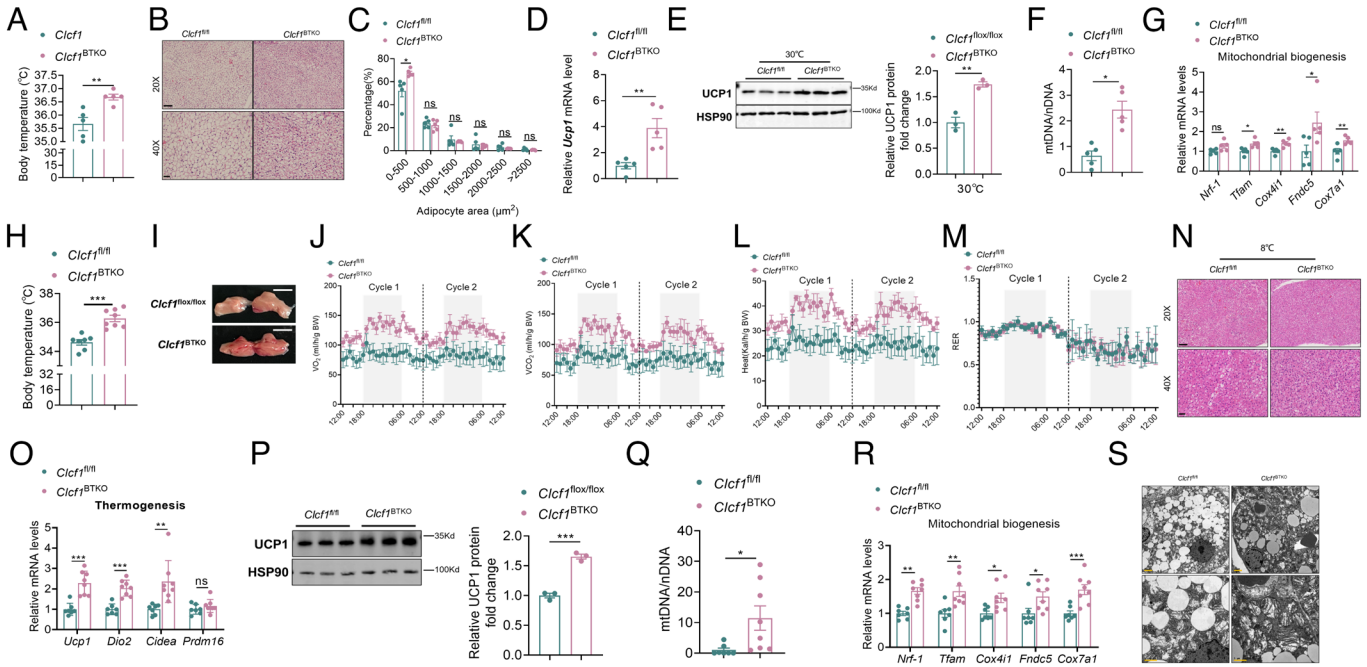

Fig. 3. CLCF1 deficiency enhances activation of BAT. (*A–G*) Ten-week-old *Clcf1*$^{fl/fl}$ mice and *Clcf1*^{BTKO} mice were housed at 30 °C for 10 d. (*A*) Core body temperatures (n = 5). (*B*) Representative H&E stains of BAT (*Top*, Scale bar, 50 μm; *Bottom*, Scale bar, 25 μm.) and (*C*) distribution of adipocyte area (n = 5). (*D*) The mRNA levels and (*E*) the protein levels (*Left*) and quantification of protein levels (*Right*) of UCP1 in BAT (*D*, n = 5; E, n = 3). (*F*) Relative mitochondrial DNA (mtDNA) levels (n = 5). (*G*) The mRNA levels of mitochondrial biogenesis genes in BAT (n = 5). (*H–S*) Eight-week-old *Clcf1*$^{fl/fl}$ mice and *Clcf1*^{BTKO} mice were exposed to 8 °C for 2 d. (*H*) Core body temperatures (n = 7 to 8). (*I*) Representative photographs of BAT. (*J*) Oxygen consumption, (*K*) carbon dioxide production, (*L*) energy expenditure, and (*M*) respiratory exchange ratio (*J–M*, n = 4). (*N*) Representative H&E stains of BAT. (*Top*, Scale bar, 50 μm; *Bottom*, Scale bar, 25 μm.) (*O*) The mRNA levels of thermogenic genes and (*P*) the protein levels (*Left*) and quantification of protein levels (*Right*) of UCP1 in BAT (*O*, n = 7 to 8; *P*, n = 3). (*Q*) Relative mitochondrial DNA (mtDNA) levels (n = 7 to 8). (*R*) The mRNA levels of mitochondrial biogenesis genes in BAT (n = 7 to 8). (*S*) Representative TEM images of mitochondria in BAT. (*Top*, Scale bar, 2 μm; *Bottom*, Scale bar, 1 μm.) Data are presented as mean ± SEM and **P* < 0.05, ***P* < 0.01, and ****P* < 0.001 by unpaired two-tailed Student's *t* tests.

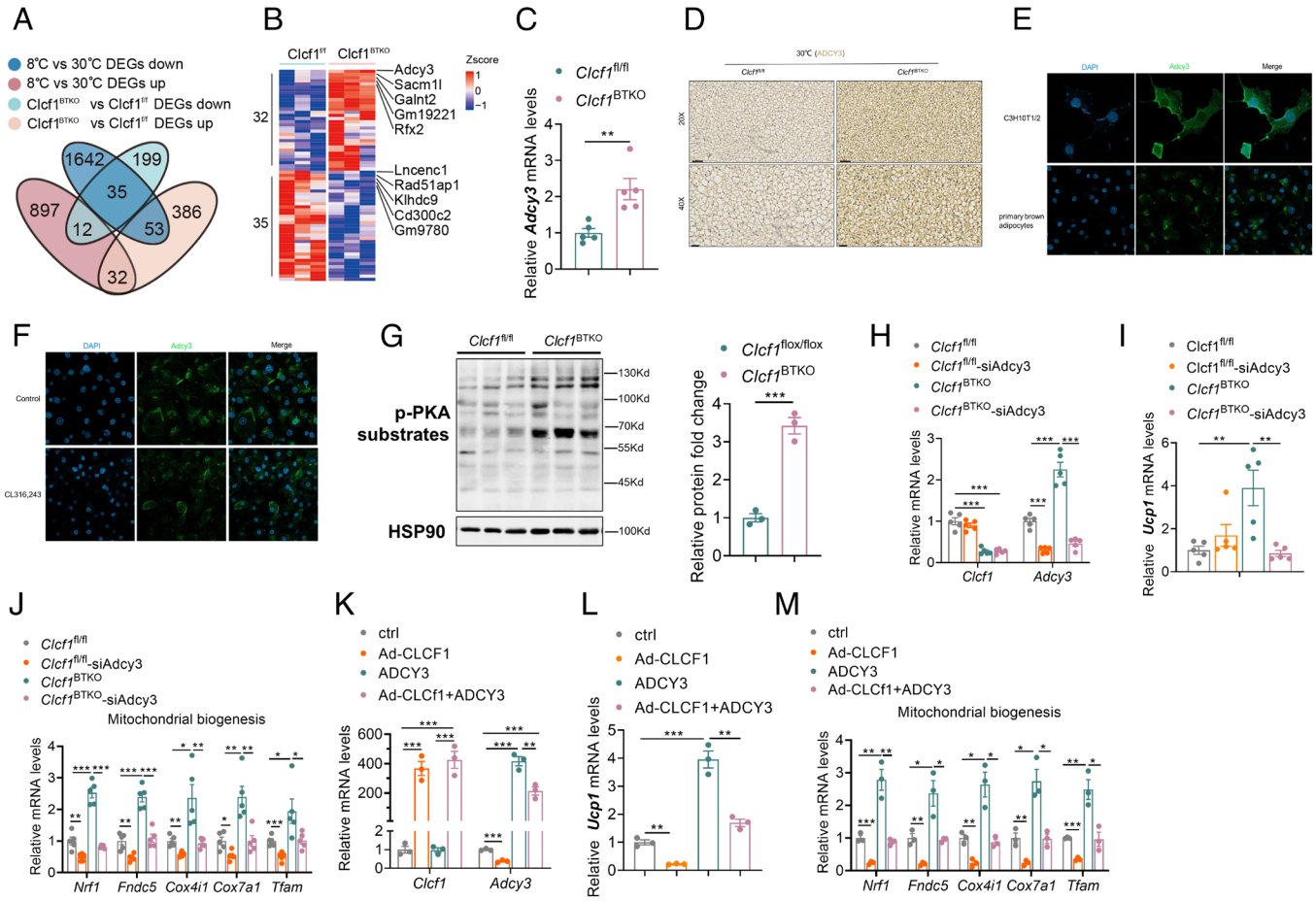

Fig. 4. *Clcf1*^{BTKO} mice up-regulate expression levels of ADCY3 to promote BAT thermogenesis. (*A*) Venn diagram of overlapped top genes from RNA-seq using total RNA extracts from BAT of *Clcf1*$^{fl/fl}$ mice and *Clcf1*^{BTKO} mice maintained at 30 °C for 10 d (n = 3) and our BAT RNA-seq from C57BL/6 mice housed at 30 °C vs. cold exposure at 8 °C for 1 d (8 °C, n = 4; 30 °C, n = 3) (|log2(Fold Change)| >1.5, *P*-value < 0.05). (*B*) Heat maps showing top-ranked genes whose expression was significantly up-regulated or down-regulated in CLCF1-deficient BAT (n = 3). (*C*) The mRNA levels of ADCY3 (n = 5) and (*D*) representative ADCY3 immunostaining (*Top*, Scale bar, 60 μm; *Bottom*, Scale bar, 30 μm.) in BAT of *Clcf1*$^{fl/fl}$ mice and *Clcf1*^{BTKO} mice maintained at 30 °C for 10 d. (*E*) Representative immunofluorescence of ADCY3 in C3H10T1/2 or primary brown adipocytes and (*F*) in primary brown adipocytes with/without CL316,243 stimulation treatment (1 μM, 6 h). (*G*) The protein levels (*Left*) and quantification of protein levels (*Right*) of PKA substrate phosphorylation in BAT of *Clcf1*$^{fl/fl}$ mice and *Clcf1*^{BTKO} mice maintained at 30 °C for 10 d (n = 3). (*H–J*) Differentiated brown adipocytes from *Clcf1*$^{fl/fl}$ mice and *Clcf1*^{BTKO} mice were transfected with ADCY3 siRNA or negative control (NC) for 48 h (n = 5 biological replicates). The mRNA levels of (*H*) CLCF1 and ADCY3, (*I*) UCP1, and (*J*) mitochondrial biogenesis genes. (*K–M*) Primary brown adipocytes from C57BL/6J mice were infected by adenovirus expressing CLCF1 (Ad-CLCF1) on day 0 and were transfected with ADCY3 expression plasmid on day 6 for 48 h (n = 3 biological replicates). The mRNA levels of (*K*) CLCF1 and ADCY3, (*L*) UCP1, and (*M*) mitochondrial biogenesis genes. Data are presented as mean ± SEM and **P* < 0.05, ***P* < 0.01, and ****P* < 0.001 by unpaired two-tailed Student's *t* tests.

Clcf1^{BTKO} mice (Fig. 4*G* and *SI Appendix*, Fig. S7*E*), while PKA signaling and ADCY3 transcription were inhibited in BAT of Ad-CLCF1-treated mice (*SI Appendix*, Fig. S7*F*).

To explore whether ADCY3 was mediating the role of CLCF1 in regulating thermogenesis, we inhibited ADCY3 expression with siRNA in isolated SVFs from BAT of *Clcf1*^{BTKO} and *Clcf1*$^{fl/fl}$ mice. After differentiation into brown adipocytes, mRNA levels of *Adcy3* were significantly increased with *Clcf1* deletion (Fig. 4*H*). *Ucp1* mRNA expression was also induced by *Clcf1* inhibition, which was reversed with combined *Clcf1* and *Adcy3* inhibition (Fig. 4*I*). Consistently, mitochondrial biogenesis–related genes, including *Nrf1, Fndc5, Cox4i1, Cox7a1, and Tfam,* showed a similar pattern with *Ucp1* (Fig. 4*J*). Next, CLCF1 or ADCY3 was overexpressed by adenovirus infection or plasmid transfection in SVFs from BAT of wild-type mice, followed by differentiation into brown adipocytes (Fig. 4*K*). The mRNA expression analysis revealed the reduced expression levels of indicated thermogenesis-related genes treated with Ad-CLCF1 (Fig. 4 *L* and *M*). Interestingly, overexpression of ADCY3 reversed the suppressive effect of *Clcf1* on mRNA expression levels of thermogenesis-related genes (Fig. 4 *L* and *M*). Thus, we conclude that ADCY3 is negatively regulated by CLCF1 signaling, and ADCY3 mediates the regulatory effect of CLCF1 in the thermogenic program in brown adipocytes.

CLCF1 Suppresses ADCY3 through the PERK-ATF4 UPR Pathway. To investigate the mechanisms of how CLCF1 negatively controls ADCY3 expression in brown adipocytes, we looked into the analyzed transcriptomic data of differentially expressed genes in BAT under cold exposure, which showed that ER stress response pathways in BAT were enriched during cold exposure (Fig. 1*B*). Further, Cnet plot analysis indicated that the activating transcription factor 4 (ATF4) pathway might be involved in both thermogenesis and the UPR pathway in BAT under cold exposure (Fig. 5*A*) (30). ATF4 is one of the key transcription factors of the UPR pathways, which is regulated by PERK activation (31, 32) and plays important roles in regulating adaptive thermogenesis (33, 34). Thus, we confirmed that ATF4 expression was increased at mRNA and protein levels under cold exposure (Fig. 5 *B* and *C*). Further, CLCF1 ablation in BAT (*Clcf1*^{BTKO} mice) indeed activated the PERK-ATF4 pathway (Fig. 5*D*), whereas CLCF1 overexpression suppressed the PERK-ATF4 pathway (Fig. 5*E*).

We hypothesized that ATF4, as a master regulator of gene expression under UPR, might be involved in regulating ADCY3 transcription with CLCF1 deficiency. Thus, we performed luciferase reporter assays with ADCY3 promoter, showing that transient ATF4 overexpression up-regulated the promoter activity of mouse ADCY3 in differentiated brown adipocytes (Fig. 5*F*). Next, we tested whether pharmacologic inhibition of PERK-ATF4 signaling could abrogate CLCF1 deficiency-induced activation of thermogenesis and energy expenditure in vitro. SVFs isolated from BAT of *Clcf1*$^{fl/fl}$ mice were treated with adenovirus harboring the recombinase (Ad-Cre) to delete CLCF1 or with GFP (Ad-GFP) as control, starting at 2 d postinitiation of differentiation. After differentiation into mature adipocytes, the primary adipocytes were treated with PERK inhibitor, GSK2606414, which blocks ATF4 expression (35). Decreased *Clcf1* mRNA levels by Ad-Cre infection and blockage of ATF4 mRNA expression by GSK260414 were confirmed by qPCR analysis (Fig. 5 *G* and *H*). The mRNA expression levels of genes related to thermogenesis, mitochondrial biogenesis, and oxygen consumption were increased upon CLCF1 deletion, which was blocked by inhibition of the ATF4 expression in differentiated brown adipocytes (Fig. 5 *I–L*). Further, oxidative phosphorylation activity in mitochondria of differentiated brown adipocytes was elevated with CLCF1 deletion, which was blocked by inhibition of ATF4 with GSK260414 treatment. To study CLCF1 signaling in adaptive thermogenesis in BAT, we tested whether CLCF1 signaling was mediated by CNTFR in brown adipocytes, which is a common receptor of the IL6 family of cytokines (21). These results indicate that ATF4 might be involved in mediating the regulation of ADCY3 by CLCF1 at both gene expression and functionality levels in BAT.

CLCF1 Suppresses the Thermogenesis of Brown Adipocytes through CNTFR. To study CLCF1 signaling in adaptive thermogenesis in BAT, we tested whether CLCF1 signaling was mediated by CNTFR in brown adipocytes, which is a common receptor of the IL6 family of cytokines (21). The mRNA levels of CNTFR were significantly higher in mature adipocytes compared to SVFs (*SI Appendix*, Fig. S8*A*), while there were no differences in mRNA levels of LIFR or gp130 (*SI Appendix*, Fig. S8 *B* and *C*). Consistent with rCLCF1, both cold exposure and CL316,243 treatment reduced CNTFR mRNA expression levels in BAT (*SI Appendix*, Fig. S8 *D* and *E*), but not LIFR or gp130 (*SI Appendix*, Fig. S8 *F–I*). Next, we inhibited CNTFR expression in differentiated brown adipocytes by siRNA (*SI Appendix*, Fig. S8*J*), which effectively abolished the recombinant CLCF1 protein (rCLCF1)-stimulated reduction of ATF4 or ADCY3 mRNA expression levels (*SI Appendix*, Fig. S8 *K* and *L*). Moreover, knocking-down of CNTFR also counteracted the inhibitory effects of rCLCF1 treatment on PKA signaling and mRNA expression of genes involved in thermogenesis and mitochondrial biogenesis

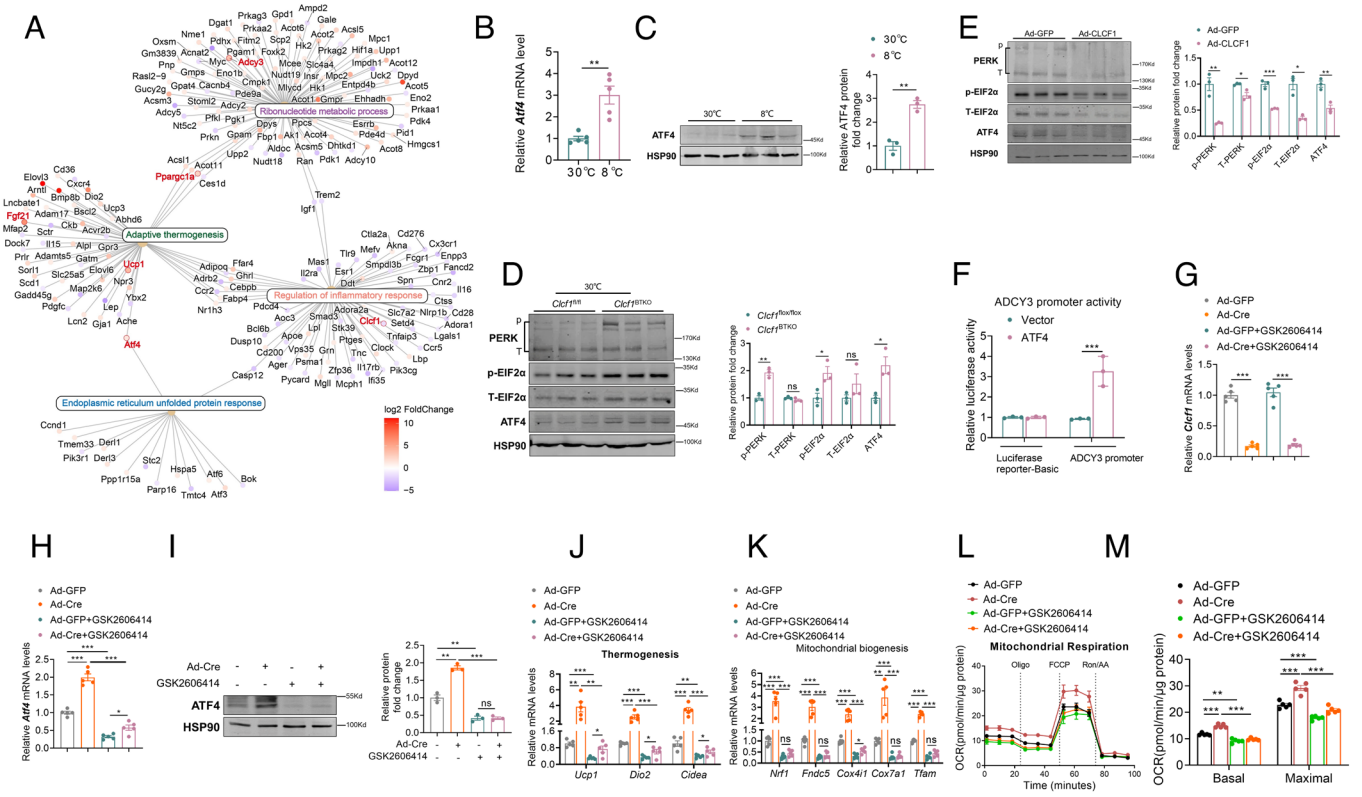

Fig. 5. *Clcf1*^{BTKO} mice activate the PERK signaling pathway regulating the transcriptional activity of ADCY3 in BAT. (*A*) GO Cnet plot analysis of BAT RNA-seq from C57BL/6 mice housed at 30 °C vs. cold exposure at 8 °C for 1 d (8 °C, n = 4; 30 °C, n = 3) (|log2(Fold Change)| >1, P_{adj} < 0.05). (*B*) The mRNA levels and (*C*) the protein levels (*Left*) and quantification of protein levels (*Right*) of ATF4 in BAT of from 8-wk-old male C57BL/6J mice housed at 30 °C or 8 °C for 1 d (*B*, n = 5; *C*, n = 3). (*D* and *E*) Western blot analysis of PERK downstream target proteins (*Left*) and quantification of protein levels (*Right*) (*D*) in BAT of *Clcf1*$^{fl/fl}$ mice and *Clcf1*^{BTKO} mice maintained at 30 °C for 10 d (n = 3) and (*E*) in BAT of Ad-GFP mice and Ad-CLCF1 mice exposed to 8 °C for 7 d (n = 3). (*F*) Luciferase reporter assays. Differentiated brown adipocytes were cotransfected with ATF4 expression plasmids and luciferase reporter plasmids containing ADCY3 promoters (n = 3 biological replicates). (*G–L*) Primary brown adipocytes from *Clcf*$^{fl/fl}$ mice were infected by adenovirus expressing Cre (Ad-Cre) on day 0 to knockout CLCF1 and were treated with PERK-specific inhibitor (GSK2606414, 1 μM) on day 7 for 48 h. (*G*) The mRNA levels of CLCF1. (*H*) The mRNA levels of ATF4. (*I*) The protein levels (*Left*) and quantification of protein levels (*Right*) of ATF4. The mRNA levels of thermogenic genes (*J*) and mitochondrial biogenesis genes (*K*). (*L*) Oxygen consumption profiles of brown adipocytes following stimulation by the indicated agents. (*M*) Bar graphs represent quantification of basal and maximal oxygen consumption (*G* and *H*, *J–M*, n = 5 biological replicates; *I*, n = 3 biological replicates). Data are presented as mean ± SEM and **P* < 0.05, ***P* < 0.01, and ****P* < 0.001. Unpaired two-tailed Student's *t* tests were performed in *B–E* and *G–K*. Two-way ANOVA tests were performed in *F* and *M*.

(*SI Appendix*, Fig. S8 *M–O*). These findings suggest that CNTFR might mediate the physiological function of CLCF1 in BAT.

CLCF1 Abrogation Alleviates Diet-Induced Obesity. To further analyze the physiological function of CLCF1 signaling under disease settings, expression levels of CLCF1 were analyzed in WT mice fed on high-fat-diet (HFD) or normal chow diet (NCD) for 12 wk. Our results showed that both mRNA and protein levels of CLCF1 were significantly increased in BAT under HFD feeding (Fig. 6 *A* and *B*). Then, *Clcf1*^{BTKO} and *Clcf1*$^{fl/fl}$ mice were fed on HFD for 16 wk, and *Clcf1*^{BTKO} mice showed more weight gain and less fat mass than the control mice without alterations in daily food intake (Fig. 6 *C–G*). Moreover, HFD-fed *Clcf1*^{BTKO} mice showed increased O_2 consumption, CO_2 emission, and heat production, as well as elevated core body temperatures (Fig. 6 *H–K*), indicating the increased energy expenditure while no difference of RER in *Clcf1*^{BTKO} mice (Fig. 6*L*). H&E staining of BAT revealed the reduced BAT mass but more multilocular lipid droplets in HFD-fed *Clcf1*^{BTKO} mice compared with the control mice (Fig. 6 *M* and *N*), while iWAT showed no apparent difference (*SI Appendix*, Fig. S9 *A* and *B*). Consistently, increased mRNA and protein levels of UCP1 in the BAT of *Clcf1*^{BTKO} mice were detected compared with the control mice (Fig. 6 *O* and *P*), whereas no difference was observed in thermogenic genes of iWAT (*SI Appendix*, Fig. S9*C*). Meanwhile, *Clcf1*^{BTKO} mice exhibited improved glucose tolerance (Fig. 6 *Q* and *R*) and insulin sensitivity (Fig. 6 *S* and *T*) compared with the control mice. Besides, the liver weight and liver to body weight ratio of *Clcf1*^{BTKO} mice fed on HFD were significantly reduced compared with the control mice (*SI Appendix*, Fig. S9 *D* and *E*). H&E staining and hepatic triglyceride quantification also showed decreased lipid accumulation in the livers of *Clcf1*^{BTKO} mice compared with the control mice (*SI Appendix*, Fig. S9 *F* and *G*), and significantly decreased mRNA levels of inflammatory genes in the liver were observed as well (*SI Appendix*, Fig. S9*H*). These results suggest that enhanced activity of BAT by inhibition of CLCF1 could protect mice from obesity-related metabolic disorders.

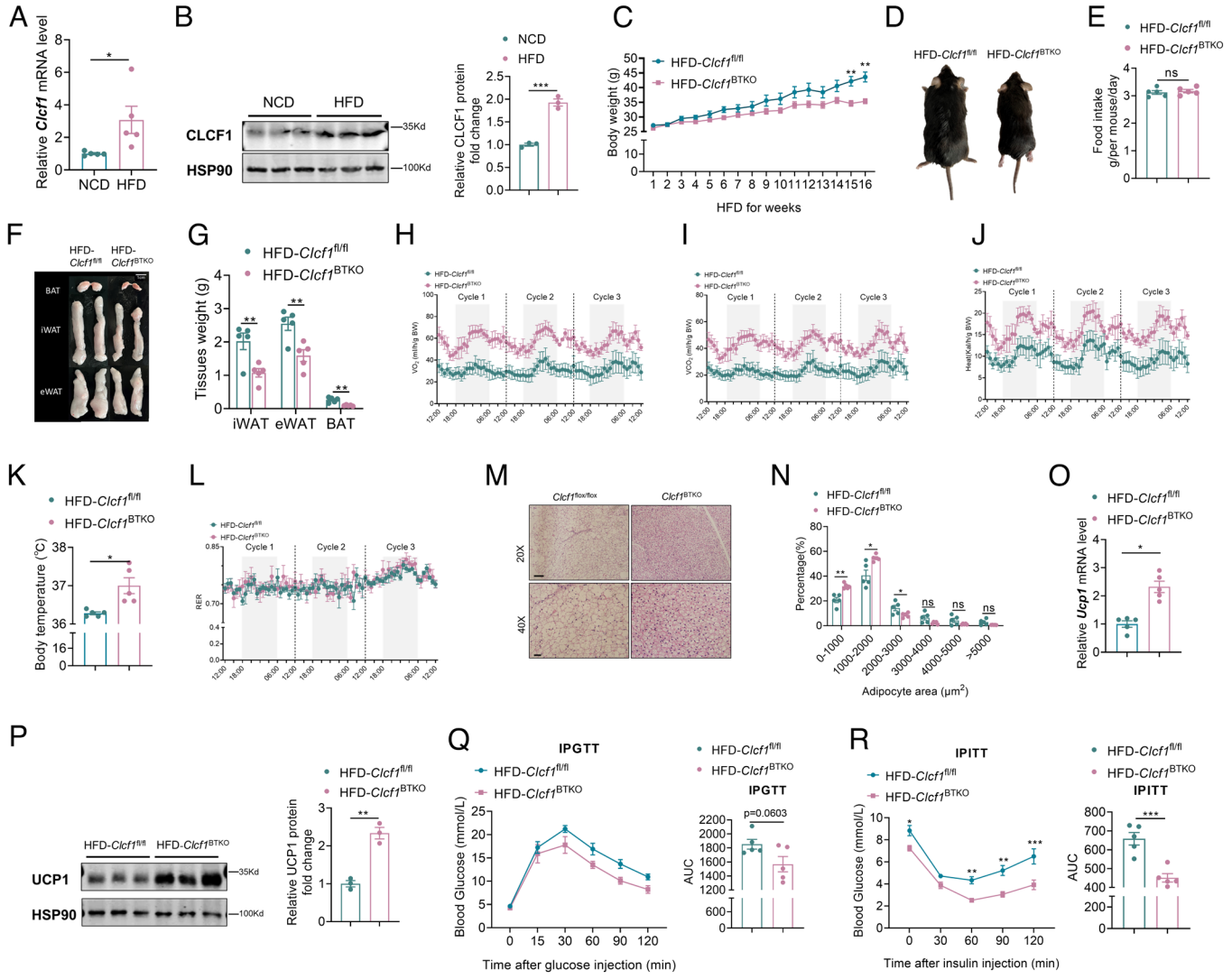

Fig. 6. *Clcf1*^{BTKO} mice increase energy expenditure and ameliorate diet-induced obesity. (*A*) The mRNA levels and (*B*) the protein levels (*Left*) and quantification of protein levels (*Right*) of CLCF1 in BAT from 8-wk-old male C57BL/6J mice fed HFD for 16 wk (n = 5). (*C–R*) Eight-week-old male *Clcf1*$^{fl/fl}$ mice and *Clcf1*^{BTKO} mice were fed NCD or HFD for 16 wk. (*C*) Body weight (n = 5). (*D*) Representative appearance of mice. (*E*) Averaged daily food intake (n = 5). (*F*) Representative photographs of BAT. (*G*) Weights of fat pads (n = 5). (*H*) Oxygen consumption, (*I*) carbon dioxide production, and (*J*) energy expenditure (n = 4). (*K*) Core body temperatures (n = 5). (*L*) Respiratory exchange ratio (n = 4). (*M*) Representative H&E stains of BAT (*Top*, Scale bar, 50 μm; *Bottom*, Scale bar, 25 μm.) and (*N*) distribution of adipocyte area (n = 5). (*O*) The mRNA levels and (*P*) the protein levels (*Left*) and quantification of protein levels (*Right*) of UCP1 in BAT (*N*, n = 5; *O*, n = 3). (*Q*) Glucose tolerance test (GTT, *Left*) and analysis of the GTT data using subtraction of basal glucose to generate an area of the curve (AOC, *Right*, n = 5). (*R*) Insulin tolerance test (ITT, *Left*) and analysis of the ITT data using AOC (*Right*, n = 5). Data are presented as mean ± SEM and **P* < 0.05, ***P* < 0.01, and ****P* < 0.001 by unpaired two-tailed Student's *t* tests.

Discussion

It has gained great attention for BAT function because of the confirmation of BAT in adult humans. Studies have shown that BAT activity was inversely correlated with body fat content or body mass index (BMI), suggesting the relationship between BAT and energy metabolism (6, 7, 36, 37). Importantly, a growing body of evidence from both animal and human studies suggests that BAT thermogenesis plays an important role in promoting energy expenditure and metabolic remodeling (4–9), which prompts us to further explore the physiological function of BAT. Notably, BAT has recently been identified as an endocrine organ, mediating metabolism in the liver, heart, muscle, etc. (5). Therefore, how to utilize the BAT adaptive thermogenesis process to promote energy expenditure and improve metabolic health has attracted increasing interest and concern. However, many factors that regulate BAT activity remain be unknown and ignored.

CLCF1 belongs to the IL-6 family of cytokines, and previous reports mainly focused on its roles in tumor progression (21, 22), but its role in metabolic homeostasis remains unclear. In this study, transcriptomic analysis revealed that CLCF1 was among the topmost affected genes of the IL6 family in BAT under cold expression in mice. Notably, other members of the IL-6 family, such as IL-6, CT1, CNTF, and LIF, have been confirmed to be involved in metabolic homeostasis, which exert antiobesity effects but mainly by acting on the central nervous system (11–16). Interestingly, a recent study showed that CLCF1 was a cholangiocyte-derived paracrine factor and played adaptive and protective roles during NASH pathogenesis (38). However, the role of CLCF1 in regulating metabolic homeostasis and whether CLCF1 could also target the central nervous system remain uncertain.

In this study, we revealed a function of CLCF1 as a negative regulator of thermogenesis in BAT. The state of energy excess such as obesity induced the expression of CLCF1 in the BAT of mice, and ectopic induction of CLCF1 expression inhibited the adaptive thermogenic program of BAT and hinders energy consumption in mice. Moreover, mice with BAT-specific knockout of CLCF1 promoted increased energy expenditure and improved metabolic disorders in mice with diet-induced obesity. Thus, blocking CLCF1 signaling by gene editing or neutralizing antibodies of CLCF1 or its receptor could be an interesting strategy to alleviate the hypercaloric state of obesity to improve metabolic parameters. For example, recent study reported a high-affinity soluble receptor (eCNTFR-Fc) blocked CLCF1 signaling and inhibited the oncogenic effects of CLCF1 in lung adenocarcinoma (21), which further suggested the possibility of targeting CLCF1 to promote energy balance in the body.

CNTFR is highly expressed in BAT, but not in iWAT, which might explain the negative effect of CLCF1 on thermogenesis in iWAT. However, we could not exclude the possibility that CLCF1 might be involved in the browning or remodeling of white adipose tissue cells under differentiation conditions. Generation of WAT-specific knockout mice or other experimental settings might help to further understand the regulatory effect of CLCF1 in thermogenesis of adipose tissues. CLCF1 and other IL-6 family members could also activate the STAT3 pathway, followed by the activation of pathways like MAPK, AMPK, mTOR, etc. (39–42). In this study, we found that CLCF1 deletion activated the PERK-ATF4 pathway in BAT. The PERK-ATF4 pathway is one of the three UPR branches regulating cellular protein homeostasis (31), which is activated in response to various cellular stressors, such as lipid toxicity or ER stress (43, 44). The signalling of PERK-ATF4 has been shown to regulate protein synthesis, lipid metabolism, mitochondrial function, etc. (45, 46). Notably, a recent study suggests that the activation of the PERK pathway contributes to mitochondrial thermogenesis in BAT (34). Furthermore, ATF4 activation in BAT helps to maintain the body temperature and attenuate obesity (33). Therefore, this study identifies the role of CLCF1 in the regulating thermogeneis through PERK-ATF4 signaling in adipose tissue. Differences in genetic manipulations, experimental settings, or tissue specificity might lead to differences in downstream signaling of CLCF1. Therefore, it could not be excluded that CLCF1 might also regulate thermogenic and energy metabolism of BAT by other pathways such as the STAT3 pathway.

Although we have identified a pathway of CLCF1 in regulating BAT thermogenesis, it should be noted that the gene expression levels of CLCF1 in BATs changed under different metabolic states. Therefore, the upstream regulatory signaling of CLCF1 remains to be explored. Recent studies showed that miR-30a-5p was directly bound to the 3′-UTR of CLCF1 mRNA to repress its protein expression, to regulate sorafenib resistance and aerobic glycolysis in liver cancer cells (47), and bromodomain-containing protein 4 (BRD4) was the transcription factor for CLCF1 in glioblastoma (48). Thus, the regulatory role of miR-30a-5p, BRD4, or other signals in CLCF1 expression in BAT remains to be investigated.

In summary, we identify the regulatory mechanism and physiological function of CLCF1 in thermogenesis in BAT and demonstrate that CLCF1 regulates the transcriptional activity of ADCY3 through the PERK-ATF4 pathway. These findings add insights into the regulation of thermogenesis in adipose tissue and provide potential therapeutic strategies against metabolic disorders.

Materials and Methods

Clcf1^{BTKO} mice were generated by intercrossing *Clcf1*$^{fl/fl}$ mice with UCP1-iCre mice. Overexpression of CLCF1 gene in BAT was achieved by adenoviral delivery. Cold exposure and thermoneutrality were performed in mice to investigate responses to adaptive thermogenesis. High-fat diet was administrated in mice to induce obesity. All other animal experiments, metabolic phenotyping studies, cell experiments, and further details regarding the materials and statistical analysis were described in *SI Appendix*.

Data, Materials, and Software Availability. The data generated in this study have been deposited in the National Center for Biotechnology Information with ID PRJNA1025828 or shown in the Dataset. All other data are included in the manuscript and/or supporting information.

ACKNOWLEDGMENTS. This study was supported by the National Key Research and Development Project (No. 2018YFA0800404), National Natural Science Foundation of China (Nos. 81970736, 82300974, and 82070811), National Science Fund for Distinguished Young Scholars (No. 82325011), the Joint Funds of the National Natural Science Foundation of China (No. U22A20288), Key-Area Clinical Research Program of Southern Medical University (Nos. LC2019ZD010 and 2019CR022), Guangdong Basic and Applied Basic Research Foundation (No. 2023A1515012202), and Guangzhou Science and Technology Plan Project (SL2024B03J00202 and 202201020497).

Author affiliations: [a]Department of Endocrinology and Metabolism, Nanfang Hospital, Southern Medical University, Guangzhou 510515, China; [b]Guangdong Provincial Key Laboratory of Shock and Microcirculation, Nanfang Hospital, Southern Medical University, Guangzhou 510515, China; [c]State Key Laboratory of Organ Failure Research, Nanfang Hospital, Southern Medical University, Guangzhou 510515, China; [d]Department of Endocrinology, Translational Research of Diabetes Key Laboratory of Chongqing Education Commission of China, The Second Affiliated Hospital of Army Medical University, Chongqing 400037, China; [e]Department of Endocrinology and Metabolism, Medical Center for Comprehensive Weight Control, The Third Affiliated Hospital of Sun Yat-sen University, Guangzhou 510630, China; and [f]Guangdong Provincial Key Laboratory of Diabetology & Guangzhou Municipal Key Laboratory of Mechanistic and Translational Obesity Research, The Third Affiliated Hospital of Sun Yat-sen University, Guangzhou 510630, China

Author contributions: G.S. and H.Z. designed research; Y.Y., K.L., X. Ye, Y.Z., F.T., and X.Z. performed research; S.W., Y.D., X. Yang, W.W., J.L., S.L., and P.Z. contributed new reagents/analytic tools; Y.Y. and K.L. analyzed data; Y.Z., F.T., X.Z., Y.D., X. Yang, W.W., J.L., S.L., and P.Z. assisted with experiments; and Y.Y., G.S., and H.Z. wrote the paper.

1. B. Cannon, J. Nedergaard, Brown adipose tissue: Function and physiological significance. *Physiol. Rev.* **84**, 277–359 (2004).
2. E. T. Chouchani, L. Kazak, B. M. Spiegelman, New advances in adaptive thermogenesis: UCP1 and beyond. *Cell Metab.* **29**, 27–37 (2019).
3. K. L. Townsend, Y. H. Tseng, Brown fat fuel utilization and thermogenesis. *Trends Endocrinol. Metab.* **25**, 168–177 (2014).
4. A. Bartelt *et al.*, Brown adipose tissue activity controls triglyceride clearance. *Nat. Med.* **17**, 200–205 (2011).
5. A. Gavaldà-Navarro, J. Villarroya, R. Cereijo, M. Giralt, F. Villarroya, The endocrine role of brown adipose tissue: An update on actors and actions. *Rev. Endocr. Metab. Disord.* **23**, 31–41 (2022).
6. A. M. Cypess *et al.*, Identification and importance of brown adipose tissue in adult humans. *N. Engl. J. Med.* **360**, 1509–1517 (2009).
7. W. D. van Marken Lichtenbelt *et al.*, Cold-activated brown adipose tissue in healthy men. *N. Engl. J. Med.* **360**, 1500–1508 (2009).
8. T. Becher *et al.*, Brown adipose tissue is associated with cardiometabolic health. *Nat. Med.* **27**, 58–65 (2021).
9. M. J. Betz, S. Enerbäck, Human brown adipose tissue: What we have learned so far. *Diabetes* **64**, 2352–2360 (2015).
10. M. Murakami, D. Kamimura, T. Hirano, Pleiotropy and specificity: Insights from the interleukin 6 family of cytokines. *Immunity* **50**, 812–831 (2019).
11. V. Wallenius *et al.*, Interleukin-6-deficient mice develop mature-onset obesity. *Nat. Med.* **8**, 75–79 (2002).
12. M. J. Moreno-Aliaga *et al.*, Cardiotrophin-1 is a key regulator of glucose and lipid metabolism. *Cell Metab.* **14**, 242–253 (2011).
13. P. D. Lambert *et al.*, Ciliary neurotrophic factor activates leptin-like pathways and reduces body fat, without cachexia or rebound weight gain, even in leptin-resistant obesity. *Proc. Natl. Acad. Sci. U.S.A.* **98**, 4652–4657 (2001).
14. M. J. Watt *et al.*, CNTF reverses obesity-induced insulin resistance by activating skeletal muscle AMPK. *Nat. Med.* **12**, 541–548 (2006).
15. E. Beretta, H. Dhillon, P. S. Kalra, S. P. Kalra, Central LIF gene therapy suppresses food intake, body weight, serum leptin and insulin for extended periods. *Peptides* **23**, 975–984 (2002).
16. G. K. Arora *et al.*, Cachexia-associated adipose loss induced by tumor-secreted leukemia inhibitory factor is counterbalanced by decreased leptin. *JCI Insight* **3**, e121221 (2018).
17. Q. Wang *et al.*, IL-27 signalling promotes adipocyte thermogenesis and energy expenditure. *Nature* **600**, 314–318 (2021).
18. Y. Yuan *et al.*, Leukemia inhibitory factor protects against liver steatosis in nonalcoholic fatty liver disease patients and obese mice. *J. Biol. Chem.* **298**, 101946 (2022).
19. G. Senaldi *et al.*, Novel neurotrophin-1/B cell-stimulating factor-3: A cytokine of the IL-6 family. *Proc. Natl. Acad. Sci. U.S.A.* **96**, 11458–11463 (1999).
20. E. Lelièvre *et al.*, Signaling pathways recruited by the cardiotrophin-like cytokine/cytokine-like factor-1 composite cytokine: Specific requirement of the membrane-bound form of ciliary neurotrophic factor receptor alpha component. *J. Biol. Chem.* **276**, 22476–22484 (2001).
21. J. W. Kim *et al.*, Antitumor activity of an engineered decoy receptor targeting CLCF1-CNTFR signaling in lung adenocarcinoma. *Nat. Med.* **25**, 1783–1795 (2019).
22. M. Song *et al.*, Cancer-associated fibroblast-mediated cellular crosstalk supports hepatocellular carcinoma progression. *Hepatology* **73**, 1717–1735 (2021).
23. A. Angius *et al.*, Exome sequencing in Crisponi/cold-induced sweating syndrome-like individuals reveals unpredicted alternative diagnoses. *Clin. Genet.* **95**, 607–614 (2019).
24. H. Li *et al.*, Peripheral IL-6/STAT3 signaling promotes beiging of white fat. *Biochim. Biophys. Acta Mol. Cell Res.* **1868**, 119080 (2021).
25. F. Shamsi, C. H. Wang, Y. H. Tseng, The evolving view of thermogenic adipocytes–Ontogeny, niche and function. *Nat. Rev. Endocrinol.* **17**, 726–744 (2021).
26. L. Wu, C. Shen, M. Seed Ahmed, C. G. Östenson, H. F. Gu, Adenylate cyclase 3: A new target for anti-obesity drug development. *Obes. Rev.* **17**, 907–914 (2016).
27. Z. Zhang *et al.*, Non-shivering thermogenesis signalling regulation and potential therapeutic applications of brown adipose tissue. *Int. J. Biol. Sci.* **17**, 2853–2870 (2021).
28. I. Barroso, ADCY3, neuronal primary cilia and obesity. *Nat. Genet.* **50**, 166–167 (2018).
29. R. E. Duncan, M. Ahmadian, K. Jaworski, E. Sarkadi-Nagy, H. S. Sul, Regulation of lipolysis in adipocytes. *Annu. Rev. Nutrition* **27**, 79–101 (2007).
30. A. M. Bolger, M. Lohse, B. Usadel, Trimmomatic: A flexible trimmer for Illumina sequence data. *Bioinformatics (Oxford, England)* **30**, 2114–2120 (2014).
31. P. Walter, D. Ron, The unfolded protein response: From stress pathway to homeostatic regulation. *Science* **334**, 1081–1086 (2011).
32. H. P. Harding *et al.*, Regulated translation initiation controls stress-induced gene expression in mammalian cells. *Mol. Cell* **6**, 1099–1108 (2000).
33. E. Paulo *et al.*, Brown adipocyte ATF4 activation improves thermoregulation and systemic metabolism. *Cell Rep.* **36**, 109742 (2021).
34. H. Kato *et al.*, ER-resident sensor PERK is essential for mitochondrial thermogenesis in brown adipose tissue. *Life Sci. Alliance* **3**, e201900576 (2020).
35. C. Meng *et al.*, PERK pathway activation promotes intracerebral hemorrhage induced secondary brain injury by inducing neuronal apoptosis both in vivo and in vitro. *Front. Neurosci.* **12**, 111 (2018).
36. M. Saito *et al.*, High incidence of metabolically active brown adipose tissue in healthy adult humans: Effects of cold exposure and adiposity. *Diabetes* **58**, 1526–1531 (2009).
37. K. A. Virtanen *et al.*, Functional brown adipose tissue in healthy adults. *N. Engl. J. Med.* **360**, 1518–1525 (2009).
38. T. Liu *et al.*, Intrahepatic paracrine signaling by cardiotrophin-like cytokine factor 1 ameliorates diet-induced NASH in mice. *Hepatology* **78**, 1478–1491 (2022), 10.1002/hep.32719.
39. J. Bollrath *et al.*, gp130-mediated Stat3 activation in enterocytes regulates cell survival and cell-cycle progression during colitis-associated tumorigenesis. *Cancer Cell* **15**, 91–102 (2009).
40. A. K. Mishra, D. Dingli, Metformin inhibits IL-6 signaling by decreasing IL-6R expression on multiple myeloma cells. *Leukemia* **33**, 2695–2709 (2019).
41. L. C. Hunt, J. White, The role of leukemia inhibitory factor receptor signaling in skeletal muscle growth, injury and disease. *Adv. Exp. Med. Biol.* **900**, 45–59 (2016).
42. S. A. Jones, B. J. Jenkins, Recent insights into targeting the IL-6 cytokine family in inflammatory diseases and cancer. *Nat. Rev. Immunol.* **18**, 773–789 (2018).
43. R. L. Wiseman, J. S. Mesgarzadeh, L. M. Hendershot, Reshaping endoplasmic reticulum quality control through the unfolded protein response. *Mol. Cell* **82**, 1477–1491 (2022).
44. C. Hetz, The unfolded protein response: Controlling cell fate decisions under ER stress and beyond. *Nat. Rev. Mol. Cell Biol.* **13**, 89–102 (2012).
45. E. Balsa *et al.*, ER And nutrient stress promote assembly of respiratory chain supercomplexes through the PERK-eIF2α axis. *Mol. Cell* **74**, 877–890.e6 (2019).
46. L. Hao *et al.*, ATF4 activation promotes hepatic mitochondrial dysfunction by repressing NRF1-TFAM signalling in alcoholic steatohepatitis. *Gut* **70**, 1933–1945 (2021).
47. Z. Zhang *et al.*, The miR-30a-5p/CLCF1 axis regulates sorafenib resistance and aerobic glycolysis in hepatocellular carcinoma. *Cell Death Dis.* **11**, 902 (2020).
48. S. H. Shen, J. F. Guo, J. Huang, Q. Zhang, Y. Cui, Bromodomain-containing protein 4 activates cardiotrophin-like cytokine factor 1, an unfavorable prognostic biomarker, and promotes glioblastoma in vitro. *Ann. Trans. Med.* **10**, 475 (2022).
49. Y. Yuan, *et al.*, CLCF1 inhibits energy expenditure via suppressing brown fat thermogenesis. National Center for Biotechnology Information. https://www.ncbi.nlm.nih.gov/sra/PRJNA1025828. Deposited 8 October 2023.